JOURNAL OF PROPULSION AND POWER
Vol. 24, No. 5, September–October 2008

Measurement of 30-Centimeter Ion Thruster Discharge Cathode Erosion

G. J. Williams Jr.*
Ohio Aerospace Institute, Cleveland, Ohio 44135
and
T. B. Smith† and A. D. Gallimore‡
University of Michigan, Ann Arbor, Michigan 48109

DOI: 10.2514/1.22982

Relative erosion rates of the discharge cathode assembly of a 30-cm ion engine are measured using laser-induced fluorescence. Molybdenum and tungsten erosion products are interrogated downstream of the discharge cathode assembly during beam extraction. Erosion of the discharge cathode assembly is characterized for both keepered and unkeepered configurations. The erosion increases with both discharge current and voltage, and spatially resolved measurements agree with observed erosion patterns. Erosion rates are calculated using data from previous wear tests. Magnitudes and trends in the rates are correlated with both previous and subsequent wear tests. Laser-induced fluorescence is demonstrated to be a technique to measure relative internal erosion rates, and a path is identified for measuring absolute rates.

Nomenclature

A_{ij}	=	Einstein A coefficient, s^{-1}
c	=	speed of light, 2.998×10^8 m/s
E_{ij}	=	energy of electronic state i with respect to state j, eV
h	=	Plank's constant, 6.626×10^{-34} Js
f_{oj}	=	oscillator strength
G	=	gaunt factor
g_i	=	degeneracy of state i
$g(\nu)$	=	Gaussian line shape, s
I	=	intensity, W/m^2
I_{SAT}	=	saturation intensity, W/m^2
J_D	=	discharge current, A
$l(\nu)$	=	power-broadened line shape, s
m_C	=	discharge cathode flow rate, sccm
m_M	=	main flow rate, sccm
n_e	=	plasma density, cm^{-3}
$n_{i,j}$	=	density of state i or j, cm^{-3}
n_o	=	ground-state density, cm^{-3}
P	=	thruster power, kW
R_{oj}	=	collisional population rate, cm^3/s
T_e	=	electron temperature, eV
TH	=	equivalent NSTAR throttle point
V_D	=	discharge voltage, V
v	=	velocity, m/s
γ	=	homogeneous relaxation rate, Hz
λ	=	wavelength, m
ν	=	frequency, Hz
σ	=	cross section, m^2

Received 4 February 2006; revision received 18 December 2007; accepted for publication 27 January 2008.

*Currently Senior Researcher, Mail Stop 16-1, NASA John H. Glenn Research Center at Lewis Field, 21000 Brookpark Road, Cleveland, OH 44116. Senior Member AIAA.

†Researcher, Dept. of Aerospace Engineering, Francois-Xavier Bagnoud Building, 1320 Beal Avenue. Senior Member AIAA.

‡Professor, Dept. of Aerospace Engineering and Applied Physics, FXB Building, 1320 Beal Avenue. Associate Fellow AIAA.

Introduction

ION thrusters are being scaled to different powers and operating conditions for space flight applications. A baseline for this scaling is the NASA Solar Electric Propulsion Technology Application Readiness (NSTAR) 30-cm ion thruster. Several wear tests on NSTAR-like hardware have been conducted to demonstrate long-duration operation and life-limiting phenomena. One of the potential failure mechanisms identified during these wear tests was erosion of the discharge cathode assembly (DCA).

Severe DCA erosion was observed in the 2000-h development wear test [1]. Posttest inspection yielded erosion rates for the tungsten outer edge of the orifice plate at 145 mm/kh and for the tip of the molybdenum cathode tube at 280 mm/kh. A keeper electrode was introduced as an engineering solution, and after a subsequent 1000-h wear test [2] and an 8200-h life demonstration test (LDT) [3], the cathode erosion was largely eliminated, whereas the keeper orifice plate (Mo) eroded in a distributed pattern, with a maximum rate of roughly 63 mm/kh near the midradius point [3]. It has been suggested that higher powers and longer periods of operation can be accommodated by thickening the orifice plates [4]. However, recent developments in cathode assembly design suggest that this would result in decreased cathode performance [5,6].

The discharge keeper orifice plate was eroded away during the NSTAR extended-life test (ELT) [7,8]. The erosion is consistent with that observed in the LDT but may have been accelerated by a shorting of the keeper to cathode potential during a segment of the test and for operation at reduced cathode current and flow rate. The rate of DCA erosion observed in the LDT would have also eroded the DCA keeper to the point that its function as a shield of the cathode orifice plate and heater was compromised by the end of the ELT. However, the loss of the keeper orifice plate did not adversely affect thruster operation in the ELT. The failure mechanism of discharge cathode erosion is the inability to maintain the discharge current or to restart [8]. Upon completion of the ELT, both the cathode orifice plate and the tip of the cathode heater were worn by charge-exchange ions, but both remained functional [9].

The source of the high-energy ions causing the erosion has remained somewhat unresolved. Ray-tracing after the 2000-h test indicated that the source of the ions was located between 1 and 11 mm downstream of the orifice plate [1]. Indeed, recent analysis has revealed that variations in sputter yield with ion angle of incidence are sufficient to reproduce the observed erosion patterns if the eroding ions originated from a point source just downstream of the DCA [10]. The cathode-to-anode potential is nominally between

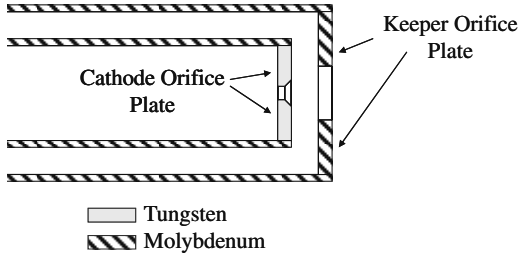

Fig. 1 Schematic of the DCA. The LIF interrogation was roughly 0.1 cm downstream (right) of both orifice plates. Note the small amount of Mo exposed on the downstream side of the cathode that encloses the cathode orifice plate.

25 and 27 V for the NSTAR thruster, and this voltage is below that required by Xe II (singly charged) ions to erode Mo at the observed rates [11]. A potential hill near the exit of the cathodes [12], sheath effects, charge-exchange collisions [13], and plasma oscillations [14] might yield high-energy Xe II ions required for the erosion [15,16]. Because Xe III (doubly charged) ions may not require these phenomena to explain the source of the erosion, they are often assumed to be the primary cause of the erosion [17]. However, recent investigations have shown backflowing Xe II ions near the face of the discharge cathode with energies sufficient to erode the cathode or keeper [15,16,18].

This paper discusses laser-induced fluorescence (LIF) erosion measurements of the DCA orifice plates. Data are correlated with operating conditions and cathode configuration.

Apparatus and Procedure

Thruster

A functional model thruster (FMT) was used in this investigation. The FMTs were the immediate predecessor to the NSTAR engineering model thrusters (EMTs), which preceded the NSTAR flight thrusters. The FMTs principally differed from the EMTs in their soft aluminum construction, as opposed to titanium for the EMTs. The magnetic field, DCA, and geometry of the discharge chamber were identical to those of the EMT-1. Quartz windows replaced roughly 20% of the anode surface and had a negligible impact on discharge chamber and thruster performance [16]. The thruster has been operated over the entire NSTAR power-throttling range. The overall performance of the thruster was comparable with the EMTs.

Figure 1 shows a schematic of the DCA in its keepered configuration. LIF data were collected along the downstream (right) faces of the orifice plates. The keeper was removed to interrogate the region near the cathode orifice plate. Note that the tungsten orifice plate is inserted in a tube of Mo. Thus, both Mo and *W* are exposed to eroding ions in the unkeepered configuration.

The ability to use wear data obtained in one test to predict those in another relies on similarity of hardware, operating conditions, and operating environment. The hardware (especially the DCA) and the operating conditions were nearly identical between this test and those of the NSTAR wear tests. The ingested flows that could modify discharge voltages or plasma density gradients of these tests are also very similar. The chambers themselves (especially, with respect to beam impingement) are somewhat different. Although the flux of backsputtered material will likely impact the observed ion optics wear rates, the small aperture sizes of the NSTAR ion optics likely precludes an impact on DCA wear. For this analysis, the impact of backsputtered material is ignored.

Measurements were made with and without the presence of a keeper electrode. Thruster operating conditions are summarized in Table 1 and correspondence to points in the NSTAR throttling table is noted [19].

Vacuum Facility

This investigation was performed in the 6×9 m Large Vacuum Test Facility at the Plasmadynamics and Electric Propulsion Laboratory with a pumping speed of 140,000 liter/s on xenon with a base pressure of less than 2×10^{-7} torr. The backpressure during 2.3-kW operation was 3×10^{-6} torr, corrected for xenon. Xenon flow was controlled to the thruster using a dedicated propellant feed system. The flow rates were periodically calibrated using a bubble flow meter. No significant variation was observed. The FMT was mounted on a two-axis positioning system with roughly 0.025-cm resolution for both stages. A 2 by 2.5 m louvered graphite panel-beam dump protected windows downstream of the thruster and reduced backsputtering from the chamber. The panels were located 4 m downstream of the thruster.

Laser and Optics

An argon-ion pumped dye laser was used in single- and multiple-beam techniques [20]. Both single- and four-beam techniques used a photovoltaic reference cell to provide a zero-velocity datum and wavelength calibration. The multiple-beam configuration was primarily used to simultaneously measure xenon ion velocity components [15], but it also yielded four simultaneous measurements of erosion at a given location. The results of the four measurements were averaged, with heavier weight given to cleaner signals. The laser was typically scanned over a 0.01-nm interval in 0.061-pm increments. The beams were delivered to the thruster in a manner identical to that used in previous Hall and ion thruster interrogations [18,20]. Alignment was facilitated by a wire crosshair on the side of the FMT plasma screen. Wavelengths associated with interrogation of the various species are given in Table 2.

Data were collected using monochromators fitted with photomultiplier tubes. Both reference and interrogation fluorescence signals were recorded via computer. The monochromator slits were set to 50 μm. Because of a 2× magnification, the effective spot size at the focus of the collection lens was 25 μm. The biconical sample volume in the cathode plume was roughly 0.5 cm long and 0.1 cm in diameter at its ends.

Several rapid (approximately 10 s) scans were taken at each data point. The rapid scans prevented long lock-in time constants from artificially broadening the fluorescence spectra and reducing the magnitude of the peak of the signal. These scans were then Chauvenet-filtered and averaged [21].

Table 1 DCA/FMT operating conditions

Designation	J_D, A	V_D, V	P, kW	m_C, sccm	m_M, sccm	TH
4 A	6.05	25.4	1.0	2.47	8.3	4
8 A	8.24	25.4	1.5	2.47	14.4	8
10 A	10.2	25.4	2.0	2.60	19.0	11
12 A, 25 V	12.1	25.1	2.3	2.90	24.0	——
12 A, 27 V	12.1	26.8	2.3	3.00	23.0	2000-h wear test
12 A, 32 V	12.1	32.2	2.3	2.65	21.0	——
12.5 A	12.6	25.4	2.2	3.10	24.0	——
13 A, 25 V	13.1	25.1	2.3	3.70	24.0	15
13 A, 27 V	13.1	26.8	2.4	2.90	24.0	——
13.5 A	13.6	25.1	2.3	3.20	24.0	——

Table 2 LIF transitions

	λ laser, nm	Term symbols (energy levels), eV	λ fluorescence, nm	Term symbols (energy levels), eV	I_{SAT}, ——
Species Mo	603.066	(1.06–2.49)	550.649	(0.93–2.49)	10
W	421.461	(0.25–2.26)	426.939	(0.25–2.27)	50

Theory

Laser-Induced Fluorescence

LIF has been used successfully in several investigations to measure the density of sputtered metals [22–25]. The principal advantages of LIF are its nonintrusiveness, high special resolution, real-time assessment, and imperviousness to conditions at the point of interrogation. Although nonintrusive at the point of interrogation, modification of the ion thruster was required to provide optical access. As already noted, the operation of the thruster was apparently unchanged, and hence the conditions at the point of interrogation are assumed to have remained unaffected.

There are several issues and challenges that have to be overcome to obtain laser-based density measurements. For the low energies associated with cathode-potential surface erosion, the vast majority of the sputtered atoms (or ions) will be in the electronic ground state. To demonstrate LIF measurement of DCA erosion, the interrogation of excited states was selected. In part, this decision was made to facilitate nearly simultaneous measurement of sputtered Mo and Xe species near the erosion site. This requires the introduction of a model that relates the population of the excited states to the ground state. This model is discussed in the next section.

Calibration of the measurement of the ground state is required to relate the measurement to the amount of metal actually sputtered. Ideally, this would be accomplished via an in situ source of known erosion rate. To reduce the scope of this investigation, the decision was made to simply correlate the observed fluorescence signal to previously measured erosion rates at identical operating conditions. The transferability of data from this experiment to previous and future operation of the thruster at identical operating conditions is necessary for the application of the results. Thus, this approach is consistent with the intent of the entire investigation.

Spatial resolution is limited by the overlap of the beam waist at the point of interrogation and the sample volume of the collection optics. For these experiments, the sample volume provided very tight resolution at the center of the sample volume, but also collected fluorescence throughout the beam. This resulted in a resolution of approximately 0.1 cm. The collection volume was centered on the laser beam waist via an alignment-pin postevacuation of the chamber. In addition to precluding resolution of the erosion to smaller than 0.1 cm, the collection volume was limited to a region a finite distance downstream of the surface that would incorporate sputtered material from a larger region of the surface.

Some fraction of the sputtered Mo or *W* may be ionized, either by the sputtering process or in the ambient plasma. However, the principal transitions of these ions are well below the tuning capability of the laser available for this investigation. In addition, several studies have indicated that the majority of the sputtered material will be neutrals [22].

Line-Shape Models

A detailed line-shape model was used to determine the temperature and Doppler shifts of the fluorescence signals [20]. Only Gaussian broadening was considered because the magnetic fields, Stark broadening, and natural line widths are negligibly small. However, because detailed spectral data were unavailable for the Mo and *W* transitions, a simpler model was employed [26]. Because the monochromator's acceptance line width was orders of magnitude greater than the laser line width (0.01 nm versus 0.0001 nm), instrument broadening was also neglected.

Neutral-density filters were periodically placed in the laser beam path to check for saturation. There was no indication of saturation during four-beam operation. However, during one-beam interrogation of Mo, the fluorescence full width at half-maximum varied significantly. Saturation intensity can be approximated by [27]

$$I_{\mathrm{SAT}} = \frac{hc}{2\sigma\lambda} \sum_{\substack{i \\ i<j}} A_{ji} \tag{1}$$

where the cross section was approximated from tabulated spectral data [28]:

$$\sigma = A_{21}\frac{\lambda^2}{8\pi} g(\nu_o)$$

The power-broadened fluorescence line shape takes the form [27]

$$l(\nu) = \frac{\gamma/2}{(\nu-\nu_o)^2 + (\gamma/2)^2(1 + I/I_{\mathrm{SAT}})} \tag{2}$$

The homogeneous relaxation rate is a combination of natural and collisional relaxation rates. These are roughly of the same order of magnitude in this investigation: $A_{ji} \approx \gamma/2$. The power-broadened line shape was convolved with a Gaussian line shape,

$$g(\nu) = \frac{c}{\nu_0}\left(\frac{m}{2\pi kT}\right)^{1/2} \exp\left[-4\,\ell_n(2)\,\frac{(\nu-\nu_0)^2}{\Delta\nu_D^2}\right] \tag{3}$$

to fit the Mo data, yielding a more accurate estimate of the temperature.

Erosion Measurements

The conversion of LIF signal to erosion rates makes several assumptions regarding the electronic state of the sputtered atoms. Although certainly proportional to the number of sputtered atoms, changes in signal strength can also result from changes in the relative population of the excited state being interrogated by the laser. For this reason, ground-state interrogation is often sought for these measurements. Unfortunately, for Mo and *W*, these states are in the ultraviolet region and are beyond the capability of the laser at hand. The electronic temperature of sputtered atoms is a function of the energy retained in the atom once sputtered and of the energy gained through interactions in the plasma near the material surfaces. The atoms are being interrogated roughly 0.1 cm from the surface, or a few microseconds after removal. This is sufficient time for the excited states to relax to ground or near-ground levels. However, collisions with ambient electrons repeatedly occur within this time, generating a distribution of excited states. Note that 0.1 cm is significantly outside of a plasma sheath on the DCA and that primary electrons, although impacting the secondary electron T_e, do not drive the excited states of the sputtered atoms.

The relative populations of the sputtered Mo and *W* atomic ground states and the lower states of the pump transitions associated with the LIF may vary with operating condition. Because of the low plasma density near the discharge cathode (particularly off-axis), assuming local thermodynamic equilibrium is not justified. A collisional-radiative equilibrium model is employed to correlate the fluorescence signal with discharge conditions [29]. In this model, the electronic states of ions are assumed to be excited by collisions (i.e., the plasma is optically thin). The states relax by radiation, because the time between collisions is significantly greater than the natural relaxation times.

For equilibrium, the rate of collisional excitation and radiative relaxation balance:

$$n_o n_e R_{o,j} = n_j A_{oj} \tag{4}$$

where the collisional population rate is [29]

$$R_{o,j} = 1.5 \times 10^{-5} \left(\frac{g_o}{g_j}\right) \frac{f_{oj}\langle G\rangle}{E_{oj} T_e^{1/2}} \tag{5}$$

However, the ratio of the population of a given excited state for two different T_e is independent of many of the terms in this equation:

$$\frac{n_i(T_{e,2})}{n_i(T_{e,1})} = \left(\frac{T_{e,2}}{T_{e,1}}\right)^{1/6} \exp\left\{\frac{E_{ij}}{T_{e,1}} - \frac{E_{ij}}{T_{e,2}}\right\} \tag{6}$$

where the temperature dependency of the terms in Eq. (5) are included. The exponential relation of excited states to ground states is still present in this relation. A full derivation of this relation can be found in [29].

The relative population of the excited states with respect to the ion's ground states was correlated with the ambient electron temperature. In situ measurement of T_e near the DCA by electrostatic probes such as Langmuir probes was beyond the scope of this investigation. However, T_e can be approximated using an empirical fit to 30-cm ion thruster data [30,31] as a function of discharge voltage V_D [32]:

$$T_e = \frac{1}{0.09} \ell_n \left(\frac{V_D}{20.0}\right) \tag{7}$$

Equation (4) predicts T_e to vary between 2.0 and 5.3 eV for discharge voltages between 24 and 32 V. Equations (2–4) were used to correct the LIF signal obtained at different discharge voltages for variations in the population of the excited state that might otherwise be interpreted as variations in the overall population of sputtered material.

Subsequent probe data taken by Herman and Gallimore [33] in the same FMT showed T_e between 2.5 and 5.0 eV across the face of the cathode keeper. Data were collected over a range of discharge currents at a roughly constant discharge voltage of 25 V. All data were collected in the keepered configuration. At the radial location of maximum keeper erosion, T_e was measured to be approximately 4 eV, compared with 2.5 eV from Eq. (4). For relative measurements at the same radial location, the absolute value of T_e is not significant for a given V_D. Because probe data were published for only one V_D, it is not clear if Eq. (4) should be modified in the argument of the natural log or in its coefficient. As discussed next, the LIF data showed significant erosion only over a small radial region of the DCA with or without a keeper. Over this range, T_e was shown to vary by less then 20%. This is of the order of the experimental error [33].

Plasma densities were also measured in these experiments. Plasma densities were found to vary from 10^{13} cm^{-3} on the centerline to 10^{11} cm^{-3} near the edges of the DCA [33]. Calculations indicate that a plasma density on the order of 10^{15} cm^{-3} is required for local thermodynamic equilibrium [16]. In this regard, the use of a collisional-radiative equilibrium approximation appears quite justified. Although a larger plasma density will impact the rate at which excited states are populated, the radiative relaxation rates remain significantly faster, and therefore no correction to the LIF signal to erosion-rate conversion is required.

LIF signals as a function of location and operating condition were converted to relative signal strengths by correcting the signal for variation in T_e. Assuming a 0.1-cm-diam sphere of interrogation 0.1 cm downstream of the DCA surface, the flux of material through this volume was calculated from a known erosion pattern assuming a less-than-cosine path of material from the surface. This "lobed" distribution has been shown to be consistent with subsequent experiments [34]. The velocity of the material was calculated from an average of LIF-measured velocimetry. The corrected relative LIF signal strengths were then converted into relative sputtered material fluxes and then into relative erosion rates.

The impacts of coatings on the eroding surfaces and of plasma oscillations were ignored. Coatings on the eroding components should be identical to beginning-of-life coatings on all contemporary NASA ion thruster components. The relation of spot measurements to integrated wear rates is a general concern and limitation of all spot measurements. Plasma oscillations were also assumed to be similar; discharge voltage and current fluctuations were similar to those observed during other NSTAR ion thruster testing. However, if the erosion was primarily due to fluctuations in the plasma (especially, because these change with operating condition), the measured rates may not reflect the integrated erosion rates.

Results

Typical Mo and *W* LIF spectra are given in Figs. 2 and 3, respectively. Reference-cell LIF data were used to assure proper laser tuning. The reference cell also provided a zero-velocity reference, primarily for Xe II velocimetry, but it yielded velocity data for the sputtered species as well [15]. The calculated velocities are roughly 1200 and 1000 m/s for Mo and *W*, respectively. However, the error in the measurement introduced by uncertainty in the frequency at the peak of the fluorescence is roughly 800 m/s.

Erosion data collected in both unkeepered and keepered configurations are presented next. Emphasis is placed on correlating the erosion rates with the discharge operating conditions. For unkeepered operation, the nominal discharge current at full power is 12.1 A and the discharge voltage is 26.8 V (referred to herein and in Table 1 as the 12-A, 27-V condition). For keepered operation, the nominal discharge current at full power is 13.1 A with a discharge voltage of 25.1 V (the 13-A, 25-V condition in Table 1). As reflected in Table 1, the NSTAR thruster was designed to be throttled below these conditions in both the unkeepered and, subsequently, the keepered configurations.

Unkeepered Configuration

Figure 4 shows Mo and *W* LIF signals as a function of radial position, as indicated by a photograph of the exit plane of the unkeepered DCA for the 12-A, 27-V operating point. Note that the

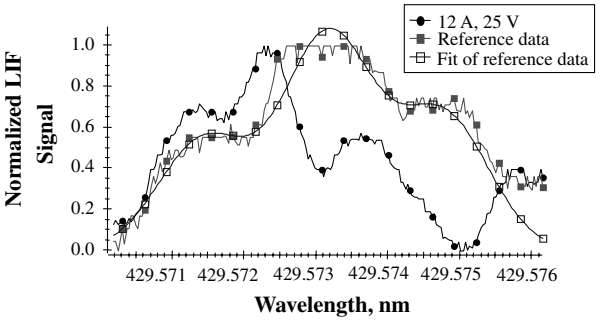

Fig. 2 Typical Mo LIF data. Note the noise in the 13-A signal compared with that obtained in the reference cell. This noise can be removed or greatly reduced by averaging several LIF scans. The offset indicates a velocity on the order of 1200 m/s.

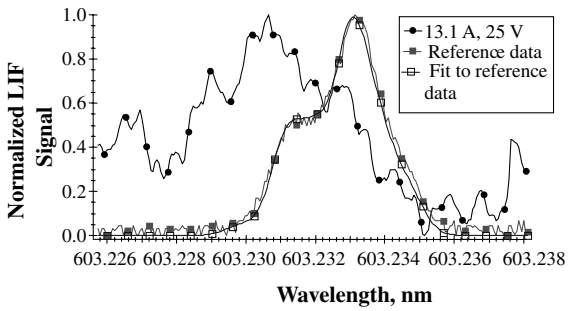

Fig. 3 Typical *W* LIF signal. Note that the slight offset of the data taken downstream of the DCA indicates an axial velocity on the order of 1000 m/s.

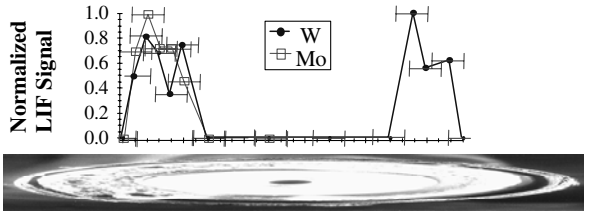

Fig. 4 Radial distribution of Mo and *W* LIF signals that were self-normalized. Note that no Mo data were taken from the right of the centerline. Data shown are for a discharge current of 12.1 A and a discharge voltage of 27 V.

signals peak at roughly the same radial position and indicate erosion peaks near the transition from the cathode orifice plate *W* to the cathode tube Mo. The resolution of the LIF technique (roughly 0.1 cm) did not allow a more detailed mapping. Horizontal error bars are provided to illustrate the uncertainty in the horizontal position. Mo data were taken over only half of the diameter. The locations of peak Mo and *W* LIF signals are in very good agreement with the observed regions of erosion. Subsequent Mo data were taken at the same location because the Mo surface subject to impinging ions is limited to this region. *W* data were taken at roughly the same point, which corresponds to the region of greatest *W* erosion in the 2000-h wear test.

Figure 5 shows the Mo LIF signal as a function of discharge current for $V_D = 25$ and 27 V. There is roughly a 50% increase in LIF signal for the higher discharge voltage. The data in Fig. 5 are corrected for saturation. Below 6 A, the signal became indistinguishable from the noise. Figures 6 and 7 show the calculated Mo and *W* erosion rates from the downstream plane of the DCA orifice plate, respectively. These points take into account the slight increase in electron temperature associated with the higher discharge voltage. Note that the Mo data showing a greater dependence on operating condition that may be an artifact of the much smaller (and noisier) *W* LIF signal, but it may also reflect tungsten's higher density and sputtering threshold. The data show average Mo sensitivities of 27 μm/kh/A and 52 μm/kh/V for a benchmark of 280 μm/kh at 12.1 A, 26.7 V (observed in the 2000-h NSTAR wear test [1]), indicating a stronger dependence on discharge voltage than on discharge current. Thus, for $J_D = 10$ A and $V_D = 25$ V, the Mo erosion rate is predicted to be

$$280 + 34 \times (10 - 12.1) + 52 \times (25 - 26.7) = 135\ \mu\text{m/kh}$$

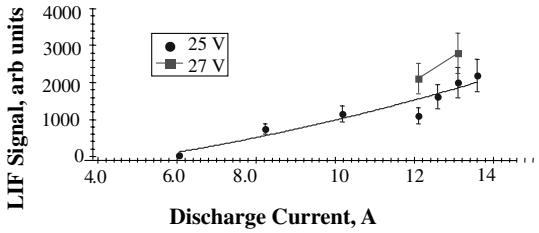

Fig. 5 Mo LIF signal as a function of discharge current for discharge voltages of 25 and 27 V for unkeepered operation. Solid lines are curve fits through the data.

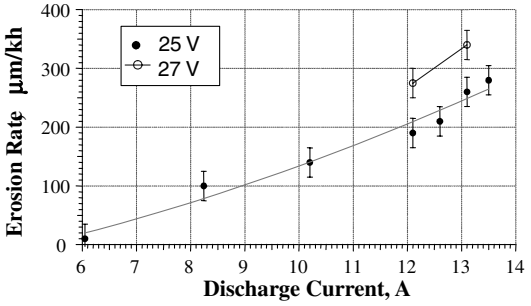

Fig. 6 Mo erosion rates of the unkeepered DCA predicted as a function of operating condition, assuming that the erosion rates observed in the 2000 h wear test were matched at the same operating condition in this test.

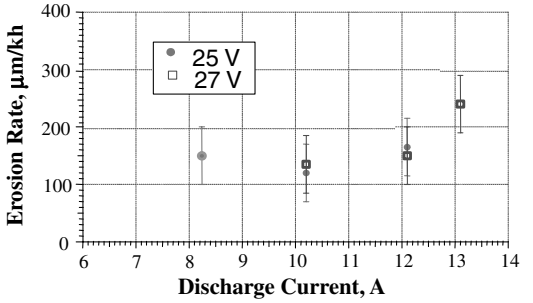

Fig. 7 Tungsten erosion rates of the unkeepered DCA predicted as a function of operating condition, assuming that the erosion rates observed in the 2000 h wear test were matched at the same operating condition in this test.

Keepered Configuration

Figure 8 shows the variation in Mo LIF signal across the face of the DCA keeper for the 13-A, 25-V operating point. The data were taken 0.05 cm downstream of the keeper orifice plate. The signal maximum is at 55% of the keeper radius. As in Fig. 4, horizontal error bars are given to reflect the uncertainty in the horizontal position. The width of the window in the discharge chamber prevented measurements beyond the edge of the keeper face. Subsequent Mo data were taken at the same radius to insure a signal at lower discharge currents. No *W* data were collected for keepered operation because the keeper is made of Mo and negligible *W* erosion was observed in unkeepered operation over the small area of the cathode orifice plate exposed during keepered operation.

Figure 9 shows the Mo LIF signal as a function of discharge current for $V_D = 25$ and 27 V. Dependence on current and voltage are again evident, and the signal is nonnegligible above $J_D = 8.2$ A.

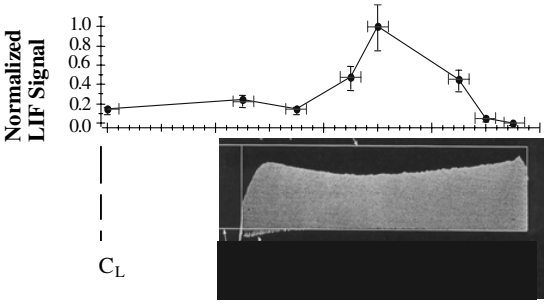

Fig. 8 Mo LIF signal across the face of the keeper electrode for 13-A, 25-V operation. Note that the signal corresponds to the erosion pattern. (The keeper photograph was taken from [3].)

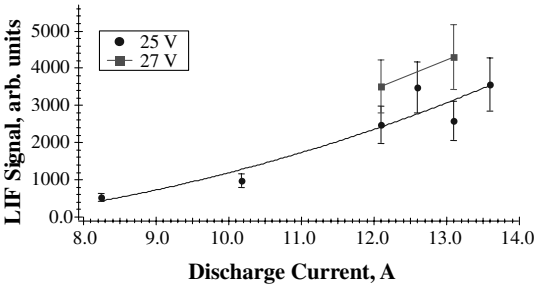

Fig. 9 Mo LIF signal as a function of discharge current for 25 and 27-V keepered operation. Solid lines are curve fits through the data.

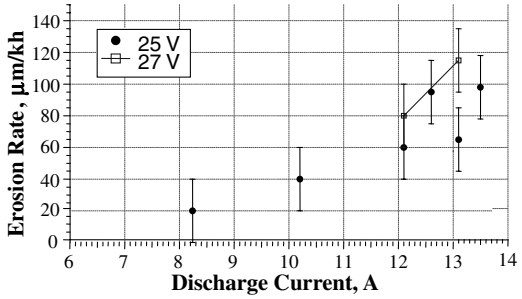

Fig. 10 Mo erosion rates of the DCA keeper predicted as a function of operating condition, assuming that the erosion rates observed in the 8200-h wear test were matched at the same operating condition in this test.

Figure 10 shows the keeper erosion rate as a function of operating condition, assuming the 13-A, 25-V case produces a rate similar to that measured in the 8200-h wear test [3]. The average sensitivities for keepered operation are roughly 14 μm/kh/A and 25 μm/kh/V for a benchmark of 63 μm/kh at 13.1 A, 25 V. Though the rates are smaller, the relative dependence on current and voltage is similar for keepered and unkeepered operations.

Sources of Experimental Error

Sources of experimental error included transition broadening due to saturation and filtering, noise in the fluorescence signal, and fluctuations in laser intensity, laser wavelength, and plasma density. The latter combined for the principal source of experimental error: noise in the fluorescence signal. The uncertainty introduced by noise in the LIF signal was roughly independent of the operating condition, yielding larger signal-to-noise ratios at higher erosion rates. The impact of broadening and saturation on erosion measurements was minimized by insuring linearity in the signal strength with laser power. Errors in temperature estimates were reduced via the saturation model. Reduction in LIF signal due to coating of the windows on the discharge chamber was accounted for by periodically measuring the relative strengths of emission lines and adjusting the LIF signal strength proportionally. Fluctuations in laser power were recorded and the data were normalized with respect to these changes. The average error was ± 20 μm/kh for Mo and ± 50 μm/kh for *W*.

Discussion

The throttling of NSTAR and post-NSTAR 30-cm ion thrusters is nominally done at a constant discharge voltage [19], which mitigates the impact of the uncertainty in T_e in calculating the rates. The gradual rise in predicted erosion rate with discharge current for both keepered and unkeepered operations is consistent with expectations. The nearly linear increase suggests that the change in erosion rate with current results largely from an increase in plasma density, rather than from a change in the local plasma structure. A nonlinear response to discharge voltage was anticipated, but time constraints precluded a detailed characterization of this response. It is anticipated that the discharge voltage will be limited to values below 28 V for chambers with Mo cathode-potential surfaces, due to screen grid erosion, and will be limited to values above 24 V, due to propellant utilization requirements (i.e., V_D is not expected to vary by more than 10%). A linear interpolation across these limits is likely sufficient.

The radial distance from the DCA centerline to the peak erosion on the keeper orifice plate is very close to the radial distance at which the *W* cathode orifice plate meets the Mo cathode tube. Because of this, it is interesting to note the differences in the erosion rates at the same location, with and without the keeper. The slight differences in operating condition suggest a 60-μm/kh reduction in Mo erosion rate of the keeper to a rate of 220 μm/kh. However, the keeper floats 3.0 V positive of the cathode at full power. The predicted Mo erosion rate would be 64 μm/kh (in excellent agreement with 63 μm/kh that was measured) if the difference in voltage was treated as a reduction in plasma potential. Given the large uncertainties in the current experiment, such agreement is fortuitous. But, assuming similar presheath ion energy distributions, it is reasonable to assume that the significant impact of the keeper voltage can be treated to first order in this way. Previous investigations have, in fact, shown the ion energy distributions in keepered and unkeepered configurations to be similar at radial distances corresponding to the maximum keeper erosion [16]. This analysis indicates that the reduced erosion observed in the 1000-h wear test and in the 8200-h LDT resulted in part from counteracting contributions of a decrease in discharge voltage and an increase in discharge current, but were largely determined by the difference in potential between the plasma and the exposed surface.

During the 32,000-h ELT, the discharge keeper revealed significant erosion during a period of midpower operation (corresponding to the 8-A point in Table 1), which was partially concurrent with the keeper shorting to the cathode [8]. Figure 10 suggests a net change in erosion rate to 102 μm/kh (including a 4-V increase in potential per the preceding discussion and ELT data [8]), which is higher than that at the previous full-power operating point (63 μm/kh), but not to the extent that one would expect a radical change in keeper wear. No data support an increase in the number of doubly charged ions at the throttled condition [7,35]; there was likely a change in the distribution of the flux of ions to the keeper. Unfortunately, the radial variation in erosion rates was not measured in this investigation except at the full-power point, due to time constraints. Equally, LIF was not used to measure the wear rates of keepers with simulated wear (e.g., with significantly larger orifices), and so it is difficult to apply the results of this study to the enlarging of the keeper orifice. However, the tungsten orifice plate was exposed to plasma for 15 kWh (no Mo was exposed on the downstream surface, following a redesign of the cathode) [8]. Data from Figs. 4 and 7 suggest that the edge of the cathode orifice plate would have been worn through in a few kilowatt hours at full power. The plate was worn through, but the thruster operating condition was varied over the 15 kWh, and so a correlation with the rate is difficult. However, the wear pattern suggests a highly nonnormal incidence for the ions because the erosion does not continue up the cathode tube.

Measurements of keeper erosion using surface-layer activation (SLA) identified trends similar to our analysis [36]. The ratio of erosion rates at the 13-A, 25-V condition to that at the 8-A condition at the same radial location was 2.8 for [2], compared with 3.2 in our investigation. Similarly, the rate for a shorted keeper at the 8-A condition was shown to be comparable with the erosion rate at the nominal/unshorted 13-A, 25-V condition. It should be noted, however, that the rates obtained using SLA were about 20 μm/kh higher than those from LIF at both operating points. This difference is within the uncertainty of the LIF measurement, but likely results from the selection of 63 μm/kh at the 13-A, 25-V operating point as the normalizing point for the erosion rates. Interestingly, the SLA analysis did show a radial variation in relative erosion rates with operating condition, but this variation was not sufficient in itself to explain the erosion observed in the ELT [36].

Another recent analysis combined optical emission spectroscopy and Cu masking to determine NSTAR keeper wear rates [17]. This analysis showed ratios in optical emission spectroscopy signals from 1.8 to 1.1 (depending on Cu wavelength) for 13-A, 25-V and 8-A operation, which are less than both LIF and SLA results. The average ratio of signal strengths at 13 A, 25 V to that at 8 A with the keeper shorted was 1.1, which is comparable with both the ratios measured using SLA and calculated from LIF data. The optical emission spectroscopy investigation indicated that the volumetric erosion observed in the ELT was consistent with previous wear tests and hypothesized that a variation in magnetic field resulted in the different wear pattern.

The introduction of graphite keepers will significantly reduce the erosion rate due to carbon's lower sputter yield. The use of graphite keepers is an engineering solution that is currently incorporated on NASA ion thrusters [37–40]. The present analysis can be adapted to graphite by appropriate scaling with density and sputter yield; however, this is complicated by the fact that the sputtering threshold

of Xe on C is significantly higher than Xe on Mo, to the extent that at 25 V, the graphite may exhibit negligible erosion.

The LIF technique can provide useful relative erosion-rate measurements on thrusters for which there is no wear-test data. However, to produce absolute rates, the measurements must be tied to actual erosion-rate measurements. Application of measured wear in one test to predict the wear in another requires the implicit assumption that erosion will be similar in different models of the same ion thruster at the same operating condition. This is true regardless of how the erosion is measured. The assumption can be removed if the erosion rate is calibrated in situ. Several methods exist to achieve this, including sputtered targets and evaporating cells [41]. It is possible that combining SLA and LIF measurements could simplify the calibration process. A large, quick matrix of erosion rates could be accomplished using LIF, and then an extended period of operation (still orders of magnitude less than a wear test) could yield an SLA profile that was periodically interrogated using LIF. Ground-state interrogation would also simplify the analysis, because variations in electronic states could be largely dismissed. The variation in electronic state could be included in the in situ calibration; otherwise, a detailed electronic state model relying on largely unknown local plasma properties would be required. In addition, a model must be developed that relates the density of sputtered material away from the surface to the actual regression rate of the surface. Replacing the transportability assumption becomes critical when the technique is applied to thrusters that have not undergone wear testing.

Conclusions

LIF was demonstrated to be a viable technique for measuring relative erosion rates of DCA surfaces. Tungsten and molybdenum species were interrogated to characterize the discharge cathode erosion process. Spatial variations in LIF signal strengths agree with measured erosion patterns. Calculated Mo and, to a lesser degree, *W* erosion rates were proportional to discharge current and discharge voltage. LIF demonstrated the sensitivity to resolve differences in erosion rate for modest changes in discharge voltage and discharge current.

The data were repeatable and comparable with other state-of-the-art erosion-rate techniques. The principal advantage of the LIF technique is that repeated real-time data can be acquired as a function of position and operating condition with the same thruster hardware. The principal disadvantage is the necessity of having optical access to the discharge chamber, which precludes measurement using high-fidelity hardware unless the beam delivery and signal collection can be accomplished through the ion optics. This may be possible, but demonstrating it was beyond the scope of the present investigation. The noise in the LIF signals can be significantly reduced using standard techniques, but these were not incorporated in the present analysis, due to time constraints. Even as is, the technique provides insight into DCA erosion that will facilitate DCA and discharge chamber development. The technique is directly extendable to other materials (e.g., carbon and barium) in the discharge chamber.

The erosion rates are consistent with observed erosion patterns in several wear tests and also agree with rates determined using surface-layer activation. The variation in rates with thruster operating condition did not explain the erosion pattern observed in the NSTAR ELT. It is likely that this resulted from a limited test matrix in the present investigation, which was completed before the results of the ELT being published. Nevertheless, the LIF technique lends itself to accommodating a very large test matrix and to characterizing both the erosion and the plasma generating the erosion in nearly simultaneous measurements.

Future application of this LIF technique would benefit from noise reduction and in situ calibration. In situ calibration, potentially of ground-state transitions, would provide an absolute measure of the eroded species, as opposed to a relative measure. The latter is limited by the need for a parallel absolute measurement such as a wear test or SLA. Indeed, the combination of LIF and SLA might provide the most cost-effective means of characterizing erosion of ion thruster components.

Acknowledgments

This research was conducted under NASA grants NAG-31572 and NAG-32216, monitored by J. Sovey. The work was made possible by the continuing support of NASA John H. Glenn Research Center at Lewis Field (GRC) and the personnel associated with the On-Board Propulsion Branch. The functional model thruster used in this investigation, along with its power console and feed system, were provided by NASA GRC. All measurements were conducted at the Plasmadynamics and Electric Propulsion Laboratory (PEPL) at the University of Michigan. The authors would like to thank the Aerospace Engineering Department's technicians and the other students in the PEPL for their assistance and support.

References

[1] Patterson, M. J., Rawlin, V. K., Sovey, J., Kussmaul, M., and Parks, J., "2.3 kW Ion Thruster Wear Test," AIAA Paper 95-2516, July 1995.

[2] Polk, J. E., Patterson, M., Brophy, J., Rawlin, V., Sovey, J., Myers, R., Blandino, J., Goodfellow, K., and Garner, C., "A 1000-Hour Wear Test of the NASA NSTAR Ion Thruster," AIAA Paper 96-2784, July 1996.

[3] Polk, J. E., Anderson, J., Brophy, J., Rawlin, V., Patterson, M., Sovey, J., and Hamley, J., "An Overview of the Results from an 8200 Hour Wear Test of the NSTAR Ion Thruster," AIAA Paper 99-2446, June 1999.

[4] Brophy, J. R., Garner, C., Polk, J., and Weiss, J., "The Ion Propulsion System on NASA's Space Technology 4/Champollion Comet Rendezvous Mission," AIAA Paper 99-2856, June 1999.

[5] Domonkos, M. T., "Evaluation of Low-Current Orificed Hollow Cathodes," Ph.D. Thesis, Univ. of Michigan, Ann Arbor, MI, Oct. 1999, pp. 153–157.

[6] Domonkos, M. T., Gallimore, A. D., and Patterson, M. J., "Parametric Investigation of Orifice Aspect-Ratio on Low Current Hollow Cathode Power Consumption," AIAA Paper 1998-3345, July 1998.

[7] Anderson, J. R., Goodfellow, K. D., Polk, J. E., Rawlin, V. K., and Sovey, J. S., "Performance Characterization of the NSTAR Ion Thruster During an On-Going Long Duration Ground Test," International Electric Propulsion Conference, Electric Rocket Propulsion Society Paper 8.0303, Mar. 2000.

[8] Sangupta, A., Brophy, J., and Goodfellow, K., "Status of the Extended Life Test of the Deep Space 1 Flight Spare Ion Engine after 25700 Hours of Operation," AIAA Paper 2003-4558, July 2003.

[9] Sengupta, A., "Destructive Physical analysis of Hollow Cathodes from the Deep Space 1 Flight Spare Ion Engine 30,000 Hr Life Test," International Electric Propulsion Conference, Electric Rocket Propulsion Society Paper 2005-026, 2005.

[10] Rovey, J. L., Gallimore, A. D., and Herman, D., "Potential Structure and Propellant Flow Rate Theory for Ion Thruster Discharge Cathode Erosion," International Electric Propulsion Conference, Electric Rocket Propulsion Society Paper 2005-022, Oct. 2005.

[11] Mantenieks, M. A., "Sputtering Threshold Energies of Heavy Ions," International Electric Propulsion Conference, Electric Rocket Propulsion Society Paper 97-187, Oct. 1997.

[12] Kameyama, I., and Wilbur, P. J., "Potential-Hill Model of High-Energy Ion Production Near High-Current Hollow Cathodes," International Symposium on Space Technology and Science Paper ISTS-98-Aa2-17, May 1998.

[13] Crofton, M. W., "The Feasibility of Hollow Cathode Ion Thrusters: A Preliminary Characterization," AIAA Paper 2000-5354, July 2000.

[14] Goebel, D. M., Jameson, K., Katz, I., and Mikellides, I., "Energetic Ion Production and Keeper Erosion in Hollow Cathode Discharges," International Electric Propulsion Conference, Electric Rocket Propulsion Society Paper 2005-266, Oct. 2005.

[15] Williams, G. J., Smith, T., and Gallimore, A., "FMT-2 Discharge Cathode Erosion Rate Measurements via Laser-Induced Fluorescence," AIAA Paper 2000-3663, July 2000.

[16] Williams, G. J., "The Use of Laser-Induced Fluorescence to Characterize Discharge Cathode Erosion in a 30 cm Ring-Cusp Ion Thruster," Ph.D. Dissertation, Univ. of Michigan, Ann Arbor, MI, 2000.

[17] Domonkos, M. T., Williams, G., Foster, J., and Patterson, M., "Investigation of Keeper Erosion in the NSTAR Ion Thruster," International Electric Propulsion Conference, Electric Rocket Propulsion Society Paper 01-308, Oct. 2001.

[18] Williams, G. J., Smith, T. B., and Gallimore, A. D., "Characterization of the FMT-2 Discharge Cathode Plume," International Electric Propulsion Conference, Electric Rocket Propulsion Society Paper 99-104, Oct. 1999.
[19] Rawlin, V. K., Sovey, J., Anderson, J., and Polk, J., "NSTAR Flight Thruster Qualification Testing," AIAA Paper 98-3936, July 1998.
[20] Williams, G. J., Gallimore, A. D., Smith, T. B., Gulczinski, F. S., Beal, B., and Drake, R. P., "Laser Induced Fluorescence Measurement of the Ion Velocity Distribution in the Plume of a Hall Thruster," AIAA Paper 99-2424, June 1999.
[21] Smith, T. B., Herman, D., Gallimore, A. D., and Drake, R. P., "Deconvolution of 2-D Velocity Distributions from Hall Thruster LIF Spectra," International Electric Propulsion Conference, Electric Rocket Propulsion Society Paper 2001-19, Oct. 2001.
[22] Gaeta, C. J., "Erosion Rate Diagnostics Using Laser-Induced Fluorescence," *Journal of Propulsion and Power*, Vol. 9, No. 3, 1993, pp. 369–376.
[23] Kovaleski, S., "Electron Beam Ablation of Materials," *Journal of Applied Physics*, Vol. 86, Dec. 1999, p. 7129.
[24] Bay, H. L., "Laser Induced Fluorescence as a Technique for Investigations of Sputtering Phenomena," *Nuclear Instruments & Methods in Physics Research, Section B*, Vol. 18, No. 1, 1987, pp. 430–445.
[25] Calaway, W. F., "Laser-Induced Fluorescence as a Tool for the Study of Ion Beam Sputtering," *Handbook of Ion Beam Processing Technology*, Noyes, Park Ridge, NJ, 1989, pp. 112–127.
[26] Williams, G. J., "Laser Induced Fluorescence Characterization of Ions Emitted from Hollow Cathodes," AIAA Paper 99-2862 June 1999.
[27] Miles, R., "Lasers and Optics," Course Notes, Princeton Univ., Princeton, NJ, 1995.
[28] Verdeyn, J. T., *Laser Electronics*, 3rd ed., Prentice–Hall, Upper Saddle River, NJ, 1995, p. 216.
[29] Huddleston, R. H., and Leonard, S. L., *Plasma Diagnostic Techniques*, Academic Press, New York, 1965 pp. 208–214.
[30] Poeschel, R. L., and Beattie, J. R., "Primary Electric Propulsion Technology Study," NASA CR-159688, 1979.
[31] Poeschel, R. L., "2.5 kW Advanced Technology Ion Thrusters," NASA CR-135076, 1976.
[32] Rock, B. A., "Development of an Optical Emission Model of the Determination of Sputtering Rates in Ion Thruster Systems," Ph.D. Dissertation, Arizona State Univ., Phoenix, AZ, 1984, pp. 43–59.
[33] Herman, D., and Gallimore, A., "Discharge Chamber Plasma Structure of a 30 cm NSTAR-type Ion Engine," AIAA Paper 2004-3792, July 2004.
[34] Yalin, A. P., Williams, J., and Zoerb, K., "Azimuthal Differential Sputter Yields of Molybdenum by Low-Energy Xe^+ Bombardment," AIAA Paper 2006-4336, July 2006.
[35] Williams, G. J., and Domonkos, M., "Measurement of Doubly Charge Ions in Ion Thruster Plumes," International Electric Propulsion Conference, Electric Rocket Propulsion Society Paper 01-310, Oct. 2001.
[36] Kolasinski, R. D., and Polk, J. E., "Characterization of Cathode Keeper Wear by Surface layer Activation," AIAA Paper 2003-5144, June 2003.
[37] Soulas, G. C., Domonkos, M., and Patterson, M., "Performance Evaluation of the NEXT Ion Engine," AIAA Paper 2003-5278, July 2003.
[38] Williams, G., Haag, T., Foster, J., Van Noord, J., Malone, S., Hickman, T., and Patterson, M., "Results of the 2000 hr Wear Test of the HiPEP Ion Thruster with Pyrolytic Graphite Ion Optics," AIAA Paper 2006-4668, July 2006.
[39] Herman, D., Soulas, G., and Patterson, M., "Status of the NEXT Ion Thruster Long Duration Test After 10,100 Jr and 207 kg Demonstrated," AIAA Paper 2007-5272, July 2007.
[40] Randolf, T., and Polk, J. E., "An Overview of the Nuclear Electric Xenon Ion System (NEXIS) Activity," AIAA Paper 2004-3450, July 2004.
[41] Domonkos, M. T., and Stevens, R. E., "Assessment of Spectroscopic, Real-Time Ion Thruster Grid Erosion Rate Measurements," AIAA Paper 2000-3815, July 2000.

R. Myers
Associate Editor